2014 IEEE International Conference on Robotics & Automation (ICRA)
Hong Kong Convention and Exhibition Center
May 31 - June 7, 2014. Hong Kong, China

Collision Free Path Planning Based on Region Clipping for Aircraft Fuel Tank Inspection Robot

Guochen Niu, Zunchao Zheng, Qingji Gao

Abstract— **Continuum robot has potential to run freely through a cluttered environment as aircraft fuel tank. To improve manual maintenance, we designed an aircraft fuel tank inspection robot which was composed of cable-driven sections. A suitable path is essential for the robot to reach the target zone while avoiding obstacles, but path planning for continuum robot is a challenge due to their complex kinematics models. To depict the collision free planning problem, a nonlinear, constrained optimization formulation was adopted. Projection strategy was presented and an imaginary straight line between the origin and the target was made up as a reference line to simplify the planning problem. We focused on the decrease of computing time complexity, and based on region clipping, a novel forward search method was proposed to solve this optimization-based planning problem. With the reference straight line, the minimum distance summation (MDS) was calculated to decide the optimal path relatively. Experiments on MATLAB were reasonably designed. Simulations and results analysis demonstrated excellent performance of region clipping search method and feasibility of the avoidance algorithm.**

I. Introduction

Fuel leakage of aircraft leads to waste of resources, high costs, and even aviation accidents. The periodical check of the aircraft fuel tank leaks is needed to guarantee the flight safety. Nowadays, tank inspection mainly depends on crews to operate internally. However, the tank distributes uniform stringers, fuel pipes and related facilities in disorder and is mixed with a few kinds of toxic gases which are flammable and explosive. In addition, the crews must follow the intricate Aircraft Maintenance Manual strictly in order to increase personnel security, so a semi-automatic device is in urgent need to improve maintenance efficiency and reduce labor intensity. To assist the crews in carrying out inspection operation, an aircraft fuel tank inspection robot (AFTIR) with continuous structure was designed [1], as shown in Fig. 1.

Some types of continuum robots like OCRobotics [2], DDU [3], Air-Octor [4], OctArm [5], Active Cannulas [6], Colobot [7], BHA [8], Tendril [9], Concentric-Tube Robots[10], etc. have been designed by researchers. Similar to snakes, elephant trunks and octopus arms, continuum robot can vary in shape and size to adapt to the environment with strong space constraints like aircraft fuel tank. In order to achieve the target in a congested space, collision free path planning is needed. Much work has been done for continuum robots moving from the starting point to the target while avoiding obstacles. G. S. Chirikjian et al. modeled hyper-redundant rigid link robots using parametric curves

Guochen Niu, Zunchao Zheng, Qingji Gao are with Robotics Institute, Civil Aviation University of China, Tianjin 300300 China. (E-mail: niu_guochen@139.com, zc.zheng.leon@gmail.com, qjgao@cauc.edu.cn).

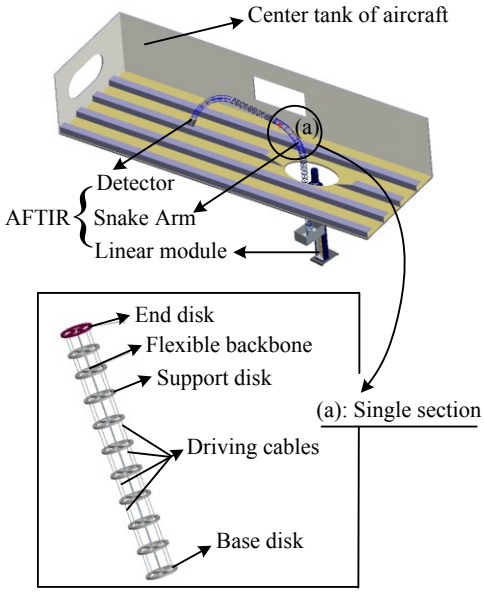

Fig.1. Pro-E simulation of AFTIR and single section (a). The structure of AFTIR mainly consists of three parts: the detector, Snake Arm and linear module. The detector percepts the environment using CCD camera, the flexible Snake Arm enters the interior of the fuel tank for inspection, and rigid linear module, the external part of fuel tank supports and provides rising and decending movements of Snake Arm. Snake Arm consists of several continuous sections. Single section consists of some support disks and one flexible backbone, and it can bend and rotate through changing lengths of four driving cables which are uniformly distributed around backbone at intervals of 90°.

approximated by mode shape functions (MSF) which was modified to apply to continuum robot [11]. L. A. Lyons et al. presented a motion planning algorithm based on optimization for an active cannula getting to the target while avoiding obstacles [12]. Penalty methods were used to solve the constrained nonlinear optimization problem by converting it into a sequence of unconstrained optimization problems. I. S. Godage et al. presented a MSFs-based kinematic model, avoiding the complex derivations and singularities [13][14]. Simulations of forward kinematics, position inverse kinematics with and without orientation, object inspection and handling, motions in static and dynamic environments demonstrated spatial bending, pure elongation/contraction and ability of avoiding obstacle. But the robot required sensors mounted around the arm to provide distal information without orientation. J. Xiao et al. designed a real-time adaptive motion planner (RAMP) for a multisection trunk/tentacle robot to grasp an object under uncertain conditions [15]. It used a planar curve parametric kinematic model to the extended RAMP paradigm. V. Duindam et al. proposed a 3D motion planning method for a bevel-tip

flexible needle in an environment with obstacles [16]. The planning problem was expressed as an optimization problem by discretizing control space and the discretization consisted of a stop-and-turn strategy and a helical strategy. But there might be no solutions for different initial estimates. The needle-tip pose probabilities generated as a diffusion process on the Euclidean group were studied. Based on Rapidly-Exploring Random Trees (RRTs) method, J. J. Xu et al. developed a motion planner for steerable needles in 3D environment with obstacles [17]. They also proposed a method using RRTs with backchaining to solve the possible problem of no solutions for all given initial configurations. These models simplified assumption which enabled us to treat the robot as particle. However, these models sacrificed accuracy for model simplicity. During medical applications, such inaccuracies could lead to significant side effects or procedure failures. R Alterovitz et al. applied a motion planning algorithm based on Rapidly-Exploring Roadmaps (RRM) to lead concentric tube robots around obstacles to goal regions [18][19]. RRM worked by minimizing the probability of colliding with obstacles. Uncertainty in actuation and predicted device shape was also accounted during plan execution.

Researches aforementioned provide obstacle avoidance path planning methods for a variety of continuum robots, but they cannot be applied directly to AFTIR due to primary differences in physical mechanisms and relative kinematics model. This paper aims to design a collision free path for AFTIR by searching solutions of fundamental kinematics using a novel method of region clipping. We emphasize the improvement of search process, for the classical blind search method is time-consuming numerously. Moreover, the introduction of projection strategy and reference straight line is used to simplify planning problem.

The structure of this paper is as follows. Based on kinematics model which has been studied on the AFTIR[20], we formulate the path planning problem in Section II. Section III details the main idea of collision avoidance strategy with region clipping search method. Design of experiments and analysis of simulation results follow in section IV.

II. PROBLEM FORMULATION

A. Kinematics Models

Through the analysis of kinematics of single section and multi-sections [20], a mapping relationship between the joint variables and tip position vector of N sections is established. The homogeneous transformation matrix (HTM) of tip frame {N} relative to system frame {0} can be expressed by (1).

$$ {}^{0}_{N}\boldsymbol{T} = {}^{0}_{1}\boldsymbol{T}\ldots{}^{i-1}_{i}\boldsymbol{T}\ldots{}^{N-1}_{N}\boldsymbol{T} \tag{1} $$

Where, ${}^{i-1}_{i}\boldsymbol{T}$ is the section frame {i} relatives to {i-1}, it is a 4×4 matrix and given by (2).

$$ {}^{i-1}_{i}\boldsymbol{T} = \begin{bmatrix} {}^{i-1}_{i}\boldsymbol{R} & {}^{i-1}_{i}\boldsymbol{p}^{T} \\ 0 & 1 \end{bmatrix} \tag{2} $$

Where, ${}^{i-1}_{i}\boldsymbol{R}$ is the rotation matrix, it is a 3×3 matrix. ${}^{i-1}_{i}\boldsymbol{p}^{T}$ is the position of the origin in frame {i} with respect to frame {i-1}, it is a 1×3 vector. The elements of ${}^{i-1}_{i}\boldsymbol{T}$ are functions of bending angle θ_i and rotation angle φ_i of i# section, they are mainly elementary operations of multiplications and additions of trigonometric functions.

We define a configuration of AFTIR as a $2N$ dimensional vector $\{\theta_i, \varphi_i: i=1,\ldots,N\}$ adding an independent translation dimension *dis*, and the arm configuration can be expressed by $\boldsymbol{q}=\{dis, \theta_i, \varphi_i: i=1,\ldots,N\}$. The function $f(\boldsymbol{q})$: $\mathbb{R}^{2N+1}\rightarrow\mathbb{R}^3$ returns the tip position $\boldsymbol{p}_{\text{tip}}$.

$$ \boldsymbol{p}_{tip} = f(\boldsymbol{q}) = [x_{tip}, y_{tip}, z_{tip}] \tag{3} $$

We define environmental obstacles using a set O of size M, $O=\{o_1,o_2,\ldots,o_M\}$, where o_i (i=1,…,M) represents i# spherical obstacle whose radius is r_0.

B. Planning Problem Formulation

Given the target point P_{target} ($\boldsymbol{p}_{\text{target}}=[x_{\text{target}},y_{\text{target}},z_{\text{target}}]$) and the initial configuration, determine an obstacle avoidance strategy that makes tip point P_{tip} (the final endpoint of the end section of Snake Arm, and $\boldsymbol{p}_{\text{tip}}=[x_{\text{tip}},y_{\text{tip}},z_{\text{tip}}]$) of AFTIR reach the target plane zone, and promise that the body of Snake Arm does not collide with obstacles and boundaries of fuel tank, and the assumptions are given as follows.

Assumption 1: The initial configuration is a status that the base of Snake Arm is on the original point in frame and the arm is perpendicular to plane *XOY*, that is, the arm is on the *Z*--axis.

Assumption 2: Reference line is a straight line from the origin to the target.

Assumption 3: Target plane zone O_1 is a circle area centered on the target in a plane parallel with plane *XOY*. Set radius of the circle as r_{target}, the zone is given as follows, where $\boldsymbol{p}$ is the coordinates variable of arbitrary point and r is the radius variable.

$$ O_1(\boldsymbol{p},r) = \left\{ \boldsymbol{p}\in R^n \left| \begin{array}{l} (x-x_{target})^2+(y-y_{target})^2 \le {r_{target}}^2 \\ z = z_{target} \end{array} \right. \right\} $$

Assumption 4: Obstacle space zone O_2 is a vertical cylinder area whose projection centre on plane *XOY* is same with that of the obstacle. An obstacle is a sphere whose centre is point P_{oba} ($\boldsymbol{p}_{\text{oba}}=[x_{\text{oba}},y_{\text{oba}},z_{\text{oba}}]$), then the obstacle space zone is given as follow formulation.

$$ O_2(\boldsymbol{p},r) = \{\boldsymbol{p}\in R^n \mid (x-x_{oba})^2+(y-y_{oba})^2 \le {r_{oba}}^2, z\ge 0\} $$

Where, r_{oba} is projection radius of obstacle space zone on plane *XOY*, $r_{\text{oba}}=r_0+r_{\text{b}}$, r_{b} is a value which is set to enlarge decision area.

Flexibility of single section and correlation between sections result in that the path planning for continuum robot is not as easy as that for a mobile robot, it cannot be taken as a particle. For this reason, the path planning problem for continuum robot can be stated as follows.

P_{tip} reaches the target while all the discrete points P_{arm} ($\boldsymbol{p}_{arm}=[x_{arm},y_{arm},z_{arm}]$) on Snake Arm do not collide with obstacle space zones, which can be represented as the constraint (4).

$$\boldsymbol{p}_{tip} \in O_1 \qquad \boldsymbol{p}_{arm} \notin O_2 \tag{4}$$

The total cost function $c(\boldsymbol{q})$ is represented by making a summation of Euclidean distances from P_{arm} on Snake Arm to the reference straight line, as expressed by (5). The distance is given by calculating exterior product of vectors $\boldsymbol{p}_{arm}$ and $\boldsymbol{p}_{target}$.

$$c(\boldsymbol{q}) = \sum d_{arm} \qquad d_{arm} = \left| \boldsymbol{p}_{arm} \times \frac{\boldsymbol{p}_{target}}{|\boldsymbol{p}_{target}|} \right| \tag{5}$$

Then path planning problem can be formulated as a nonlinear, constrained optimization problem as follows.

$$\boldsymbol{q}^* = \arg\min c(\boldsymbol{q}), \text{ subject to: } \boldsymbol{p}_{tip} \in O_1,\ \boldsymbol{p}_{arm} \notin O_2 \tag{6}$$

Where $\boldsymbol{q}^*$ is the optimal solution path.

III. Obstacle Avoidance Strategy

A. Projection Strategy

Figure 2 shows the part environment in the wing tank of Boeing 737-200, the uniform stringers, fuel pipes and other facilities distributes in disorder.

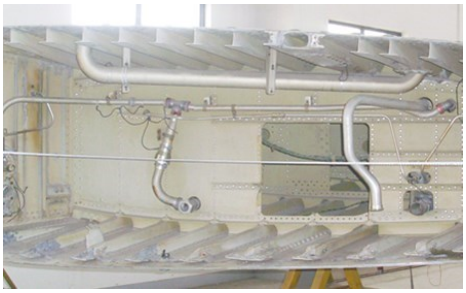

Fig.2. The internal environment of wing tank of Boeing 737-200.

With obstacles in space, there may be more than one solution path for AFTIR to reach the same target. So, to simplify the planning problem, we also present the assumption of target space zone as that in the former section.

Assumption 5: Target space zone O_3 is a vertical cylinder area whose projection on plane *XOY* is a circle centered on the target. It can be formulated as follow form.

$$O_3(\boldsymbol{p},r) = \{\boldsymbol{p} \in R^n \mid (x-x_{target})^2 + (y-y_{target})^2 \le r_{target}{}^2, z \ge 0\}$$

With above assumptions, the projection strategy is applied as follows. As shown in Fig. 3 and Fig. 4, firstly, with an initial configuration, the Snake Arm bends and rotates until the tip point reaches the target space zone, and make sure that any parts of the arm do not run into obstacle space zones. Then the arm rises or descends a distance until the tip point is in the target plane zone, and no matter how the body moves upward or downward, it does not collide with obstacles. In this way, the fuel pipe can be considered as a sequence of obstacles arranged vertically, that is, avoiding one obstacle means avoiding a vertical pipe standing where the obstacle is.

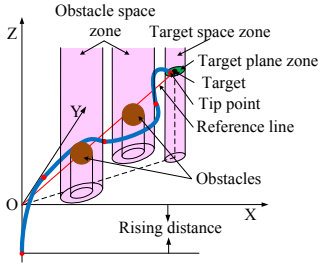

Fig. 3. Diagram of a path of four sections avoiding two obstacles with projection strategy.

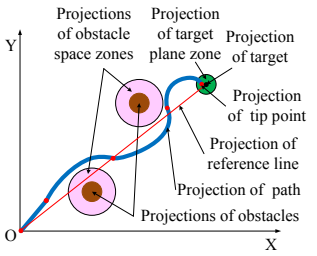

Fig. 4. Projections in plane *XOY* of shapes in Fig. 3.

B. Region Clipping Search Method

The analysis of continuity of functions based on forward kinematics is precondition of introducing region clipping which is a forward research method with low computing time complexity. On the basis of kinematics modeled in [20], we give the following analysis.

For a single section, define $\boldsymbol{p}_{Nr}$ (N is the number of sections, N=1 means the arm is a single section, L is the length of single section, l represents a distance from a point on the section to the base of the section, $l \ge 0$, $l \le L$) as an arbitrary point on the body and the corresponding bending angle is α ($\alpha = l*\theta/L$). So, the position vector of $\boldsymbol{p}_{1l}=[x_{1l},y_{1l},z_{1l}]$ is given by $\boldsymbol{p}_{Nr}=[x_{Nl},y_{Nl},z_{Nl}]$ (N=1) when $\theta \in [-\pi,0) \cup (0,\pi]$, $\varphi \in [0,2\pi]$, and where

$$\begin{cases} x_{1l} = \dfrac{L}{\theta}\cos\varphi(1-\cos\alpha) \\ y_{1l} = \dfrac{L}{\theta}\sin\varphi(1-\cos\alpha) \\ z_{1l} = \dfrac{L}{\theta}\sin(\alpha) \end{cases} \tag{7}$$

Equation (7) indicates that, if we make θ or φ to be a known constant, so x_{1l}, y_{1l}, and z_{1l} can be taken as unary functions of φ or θ, moreover, they are also complex functions of multiple elementary functions. For an arbitrary $\varphi=\varphi_0$, if θ tends to zero, that is, α tends to zero, we have (8).

$$\begin{cases} \lim\limits_{\theta\to 0} x_{1l} = 0 = x_{1l}(\theta,\varphi) \mid \theta = 0, \varphi = \varphi_0 \\ \lim\limits_{\theta\to 0} y_{1l} = 0 = y_{1l}(\theta,\varphi) \mid \theta = 0, \varphi = \varphi_0 \\ \lim\limits_{\theta\to 0} z_{1l} = l = z_{1l}(\theta,\varphi) \mid \theta = 0, \varphi = \varphi_0 \end{cases} \tag{8}$$

By the definition of continuity of unary function [21], we can consider elementary functions x_{1l}, y_{1l}, z_{1l} are unary functions if a variable is made as constant, so they are surely continuous functions, that is, if θ is constant, position function of single section is continuous for φ in interval of $[0,2\pi]$. Or if φ is constant, position function of single section is continuous for θ in interval of $[-\pi,\pi]$.

For multi-sections, as ${}_N^0\boldsymbol{T}$ in (2) is got by a product of N matrices, $\boldsymbol{p}_{NL}$ (the tip position $\boldsymbol{p}_{\text{tip}}$) is formulated by the multiplications and additions of elements of N matrices, the element of ${}_N^0\boldsymbol{T}$ is function of $\{\theta_1,\varphi_1,\theta_2,\varphi_2,\ldots,\theta_N,\varphi_N\}$.

Take an example of bending angle, for a combination of $\{\theta_1,\varphi_1,\theta_2,\varphi_2,\ldots,\theta_N,\varphi_N\}$, we choose an value θ_i arbitrarily as an independent variable θ and the others as known constants. In this way, (2) can be given by function form (9).

$$ {}_N^0\boldsymbol{T}(\theta) = {}_1^0\boldsymbol{T}(\theta_1,\varphi_1)\ldots{}_i^{i-1}\boldsymbol{T}(\theta,\varphi_i)\ldots{}_N^{N-1}\boldsymbol{T}(\theta_N,\varphi_N) \tag{9}$$

Where,

$$ {}_j^{j-1}\boldsymbol{T}\left(\theta_j,\varphi_j\right)=\begin{bmatrix} {}_j^{j-1}f_{11}\left(\theta_j,\varphi_j\right) & \ldots & {}_j^{j-1}f_{14}\left(\theta_j,\varphi_j\right) \\ \vdots & \ddots & \vdots \\ {}_j^{j-1}f_{41}\left(\theta_j,\varphi_j\right) & \ldots & {}_j^{j-1}f_{44}\left(\theta_j,\varphi_j\right) \end{bmatrix}. $$

The elements of $\boldsymbol{T}$ are taken as functions $f_{mn}(\theta)$ (m=1,2,3,4; n=1,2,3,4), the subscript mn represents its position of the matrix $\boldsymbol{T}$, the m-th row and n-th column. From (2), $\boldsymbol{p}_{NL}$ can be given by (10).

$$ \boldsymbol{p}_{NL}=\left[x_{NL},y_{NL},z_{NL}\right]=\left[{}_N^0f_{14}(\theta),\ {}_N^0f_{24}(\theta),\ {}_N^0f_{34}(\theta)\right] \tag{10}$$

Where ${}_N^0f(\theta)$ can be regarded as unary function of θ through operation combinations of elements of ${}_j^{j-1}\boldsymbol{T}$ (j=1,2,…,N), as given by (11). Clearly, it is continuous for θ in an interval of $[-\pi,\pi]$.

$$ \begin{aligned} {}_N^0f_{k4}\left(\theta\right) = g\Big[&{}_1^0f_{mn}\left(\theta_1,\varphi_1\right),\ldots,{}_{i-1}^{i-2}f_{mn}\left(\theta_{i-1},\varphi_{i-1}\right),\ldots \\ &\ldots,{}_i^{i-1}f_{mn}\left(\theta,\varphi_i\right),{}_{i+1}^{i}f_{mn}\left(\theta_{i+1},\varphi_{i+1}\right),\ldots,{}_N^{N-1}f_{mn}\left(\theta_N,\varphi_N\right)\Big] \\ &k=1,2,3;\quad m=1,2,3,4;\quad n=1,2,3,4 \end{aligned} \tag{11}$$

Where ${}_N^0f_{k4}\left(\theta\right)$ is a function of θ with an operation combination which is elementary operation of multiplications and additions of ${}_j^{j-1}f_{mn}$ (j=1,2,…,N) which represents any elements of ${}_j^{j-1}\boldsymbol{T}$ (j=1,2,…,N).

By the definition of continuous unary function according to [21], we could imply from (11) as follows.

$\forall\varepsilon>0$, $\exists\Delta\theta>0$, s.t $\left|{}_N^0f_{k4}\left(\theta\right)-{}_N^0f_{k4}\left(\theta_0\right)\right|<\varepsilon$, for $\forall\theta\in O\left(\theta_0,\Delta\theta\right)$.

In another way, for θ_0 (θ_0 represents the value of bending angle of i# section, with a known combination $\{\theta_1,\varphi_1,\ldots,\theta_{i-1},\varphi_{i-1},\theta,\varphi_i,\theta_{i+1},\varphi_{i+1},\ldots,\theta_N,\varphi_N\}$) corresponds a tip point $[x_{\text{NL}}(\theta_0),y_{NL}(\theta_0),z_{NL}(\theta_0)]$ which is in target space zone, when the variable θ changes by $\Delta\theta$ and $\Delta\theta$ tends to zero, we have conclusions as (12).

$$ \lim_{\Delta\theta\to0}\Delta x_{NL}=0,\ \lim_{\Delta\theta\to0}\Delta y_{NL}=0,\ \lim_{\Delta\theta\to0}\Delta z_{NL}=0 \tag{12}$$

So for the position change Δd on the direction of vector $[\Delta x_{NL},\Delta y_{NL},\Delta z_{NL}]$, we have (13).

$$ \begin{aligned} \lim_{\Delta\theta\to0}\Delta d &= \left|\left(\Delta x_{NL}{}^2+\Delta y_{NL}{}^2+\Delta z_{NL}{}^2\right)^{\frac{1}{2}}\right| \\ &= \left(\lim_{\Delta\theta\to0}\Delta x_{NL}{}^2+\lim_{\Delta\theta\to0}\Delta y_{NL}{}^2+\lim_{\Delta\theta\to0}\Delta z_{NL}{}^2\right)^{\frac{1}{2}} \\ &= 0 \end{aligned} \tag{13}$$

From (12) and (13), we know that when θ changes nearby θ_0, tip point moves nearby tip point $[x_{\text{NL}}(\theta_0),y_{NL}(\theta_0),z_{NL}(\theta_0)]$, that is, the tip point changes near the target space zone in a direction of vector $[\Delta x_{NL},\Delta y_{NL},\Delta z_{NL}]$.

We can conclude a similar result with rotation angle, as illation of bending angle above-mentioned when choosing an value φ_{i} arbitrarily as an independent variable φ and the others as known constants, they form a combination of $\{\theta_1,\varphi_1,\ldots,\theta_{\text{i-1}},\varphi_{\text{i-1}},\theta_i,\varphi,\theta_{i+1},\varphi_{i+1},\ldots,\theta_N,\varphi_N\}$.

In conclusion, continuity means the position coordinates of $\boldsymbol{p}_{NL}$ are distributed continuously in their own direction of coordinate axis, or, continuity analysis of unary functions presents relation between changes of any angle and movements of tip point, that is, the position of tip point changes gradually, other than mutationally. In another way, as long as a solution making the tip point in the target space zone is found, we can always find a more suitable solution near the known angles by small angle changes, until the optimal one is found and tip point is not aside to target space zone.

Blind search method searches many inessential angles, and it leads to large computing time. Considering the distribution of feasible values got from blind search, a novel search method of region clipping is proposed to reduce computing time.

The main idea comes from the analysis of continuity of HTM, and it aims to reserve useful regions and remove the useless regions through searching less value continually. As shown in Fig. 5, take an example of bending angle, firstly we divided the interval of θ into NUM parts averagely and get NUM+1 values in the searching region (NUM is usually a small integer, in Fig. 5, NUM=8), and we get a series of combinations of bending angles $\{\theta_i(1),\ldots,\theta_i(9)\}$ (i=1,2,…,N) for i# section. Through calculating the tip coordinates, if it satisfies reaching the target space zone, keep it. Secondly, we choose an optimal value $\{\theta_1(7),\ldots,\theta_N(4)\}$ which is calculated from minimum distance summation(MDS) which is the minimum summation of distances from all points of Snake Arm to the reference straight line, and make its prior value $\{\theta_1(6),\ldots,\theta_N(3)\}$ and its later one $\{\theta_1(8),\ldots,\theta_N(5)\}$ as left and right endpoints of the next searching regions of $\{\theta_1,\ldots,\theta_N\}$. Finally, the loop stops when the angle changes less than a pre-set small angle $\Delta\theta$, that is, double length of subinterval in the last loop but one is less than $\Delta\theta$. The relation among length of initial interval Li, number of loops $LOOP$, NUM and $\Delta\theta$ is given by (14).

$$ Li\times\left(\frac{2}{NUM}\right)^{LOOP-1}\le\Delta\theta \tag{14}$$

In this way, 8 of 9 values and 6 of 8 subsections will be abandoned in the next loop, and *LOOP*=7 in the figure is $(\pi\times(2/8)^{LOOP-1}\leq\pi/1800$ when we make $\Delta\theta$=0.1°).

Just like a tailor, most of searching regions are clipped in each loop until the optimal value is obtained, so we do not need to calculate numerous unnecessary values, and get a low computing time complexity at the same time.

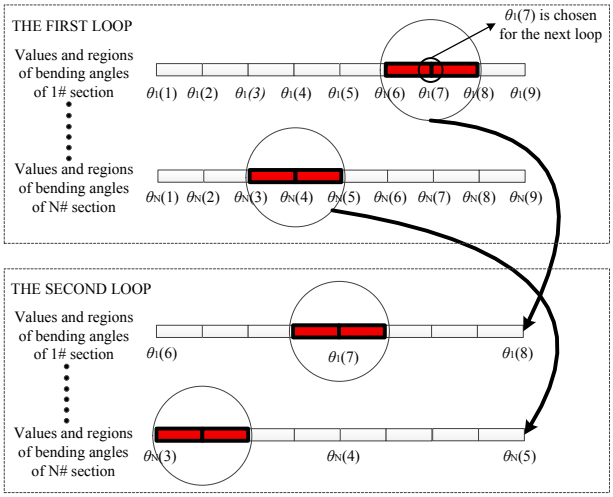

Fig. 5. Principle of region clipping search method and the red regions are reserved in each loop, where the red subintervals are chosen in each loop.

C. Algorithm Details

For path planning in a 3D space, the optimal path from the starting point to the target is clearly the straight line between them. Considering special characteristics of continuum robot, we use the fictitious straight line as reference and adopt a planning method based on projection strategy and region clipping search method, and obtain the optimal result through calculating MDS in every loop, the process of minimizing MDSs is the process of solving the nonlinear constrained optimization. The algorithm details as follows.

As shown in TABLE I, initialize the configurations firstly, and input the starting point P_{init} and the target point P_{target}. Imagining firstly there is a straight line between original point and P_{target}. Starting with the movement of 1# section, we divide each domain of θ_1 and φ_1 into *NUM* parts then we get two sets of $\Theta=\{\theta_1(1),\ldots,\theta_1(NUM+1)\}$ and $\Phi=\{\varphi_1(1),\ldots,\varphi_1(NUM+1)\}$. All combinations of $\{\theta_1(i),\varphi_1(j):i,j=1,2,\ldots,NUM+1\}$ is formed and used to calculate the pose of 1# section. Then the Collision Detection runs, that is, if the single section does not collide with obstacle space zone, keep the combination of $\{\theta_1(i), \varphi_1(j)\}$, or omit it. Reaching Detection works with $\{\theta_1(i), \varphi_1(j)\}$ chosen above, that is, we compute the corresponding tip position of 1# section, if the tip is not in the target space zone, 2# section is added. In the same way, we divide the domains and choose the solutions that with known $\{\theta_1(i), \varphi_1(j)\}$got in former loop through Collision Detection and Reaching Detection. The number of active sections is added until the tip of Snake Arm reaches the target space zone. With each combination of $\{\theta_1,\varphi_1,\ldots,\theta_N,\varphi_N\}$ satisfying conditions of reaching target space zone, then we calculate the rising distance by moving the arm up or down to make the tip in the target plane zone, in this way, paths of configurations $\boldsymbol{q}=\{dis,\theta_i,\varphi_i:i=1,\ldots,N\}$ are obtained. There is a corresponding summation of distances from discrete points along the sections to the reference straight line for every path, and the minimum one of summations is calculated, that is MDS. After choosing MDS, we divide the corresponding interval of each angle of $\{\theta_i,\varphi_i:i=1,\ldots,N\}$ and compute the best configuration until (14) is satisfied. Finally, the optimal path with configuration corresponding $\boldsymbol{q}=\{dis,\theta_i,\varphi_i:i=1,\ldots,N\}$ is obtained.

TABLE I. PROGRAMING DESIGN OF PATH PLANNING

OBASTACLE_AVIODANCE_PROCEDURE(P_{init},P_{target},O_{oba})
1. DEFINE O_1 as a target plane zone
2. DEFINE O_2 as obstacle space zones
3. DEFINE O_3 as a target space zone
4. DEFINE P_{tip} as tip point of Snake Arm
5. DRAW_REFERENCE_LINE(P_{init},P_{target})
6. Θ and Φ←REGION_COLIIPING (1)
7. $\boldsymbol{q}_1=\{\theta_1(i),\varphi_1(j)\}$←COLLISION_DETECTION (Θ,Φ)
8. $\boldsymbol{q}=\{dis,\theta_1,\varphi_1\}$←REACHING_DETECTION ($\boldsymbol{q}_1$)
9. CALCULATE MDSs
10. While Equation (14) is not satisfied
11. ADD a section
12. REPEAT step 6-11 with an added section
13. END
14. RETURN optimal $\boldsymbol{q}=\{dis,\theta_i,\varphi_i:i=1,2,\ldots,N\}$

REGION_COLIPPING (i)
1. INPUT i# section
2. DIVIDE interval of each angle of $\boldsymbol{q}=(\theta_i, \varphi_i$:i=1,…,$N)$
3. EACH interval has *NUM* subintervals
4. RETURN Θ={θ_1(1), ,…, θ_1(*NUM*+1) } and Φ={φ_1(1),…,φ_1(*NUM*+1)}

COLLISION_DETECTION (Θ,Φ)
1. COMBINE the elements of Θ with that of Φ
2. GET combinations of $\boldsymbol{q}_i=\{\theta_1,\varphi_1,\ldots,\theta_i,\varphi_i\}$
3. CALCULATE the poses of $\boldsymbol{q}_i$
4. If the arm does not collide with O_2
5. Keep $\boldsymbol{q}_i$
6. Else
7. CALCULATE next $\boldsymbol{q}_i$
8. RETURN $\boldsymbol{q}_i$

REACHING_DETECTION ($\boldsymbol{q}_i$)
1. CALCULATE P_{tip} of $\boldsymbol{q}_i$
2. If $P_{tip}\cap O_3\neq\varnothing$
3. Save $\boldsymbol{q}_i$ and calculate rising distance
4. Else
5. CALCULATE P_{tip} of next $\boldsymbol{q}_i$
6. RETURN $\boldsymbol{q}=\{dis,\theta_i,\varphi_i$:i=1,2,…,N}

The procedure of REGION_COLIPPING() is designed to divide the intervals of angles. The procedure of COLLISION_DETECTION() aims to judge whether the Snake Arm collides with obstacles or not. The procedure of REACHING_DETECTION() keeps the configurations that satisfying the conditions of the tip reaches the target plane zone when the number of active sections is *i*.

IV. SIMULATION DESIGN AND RESULTS ANALYSIS

A. Experiments Design

Take an example of collision free path planning for a target [30,18,51], and we need three sections. In this experiment, we set the radius of spherical obstacle r_0=2cm, r_b=2cm, and r_{oba}=3cm, r_{target}=1cm, *L*=25cm, $\Delta\theta$=0.1°, *NUM*=10. The design of experiments is as follows.

(1). Plan a path without obstacles or with obstacles that locates far from the origin and the target, which has no effect on the path. For example, path planned in an environment without obstacles, as shown in Fig. 6(a).

(2). Choose a point [3.90,2.25,5.45] near the first section of path in Fig. 6(a), 1# obstacle is centered on the chosen point, and the path avoiding 1# obstacle is depicted in Fig. 6(b).

(3). Choose another point [6.15,10.67,23.86] on the second section of path in Fig. 6(b), 2# obstacle is centered on this second point, and a path avoiding 1# and 2# obstacles is given in Fig. 6(c).

(4). Choose a third point [21.34,14.93,43.35] on the third section of path in Fig. 6(c), 3# obstacle is centered on this point, and a path avoiding 1#, 2# and 3# obstacles is shown in Fig. 6(d).

(5). Views of all the figures are the same one.

Data of experiments (1)-(4) are shown in TABLE II. The way we choose obstacles guarantees the obstacles have certain effect on the path, for the collision free method requires searching solutions consecutively. In this way, the path planning with special obstacle chosen indicates feasibility of obstacle avoidance strategy.

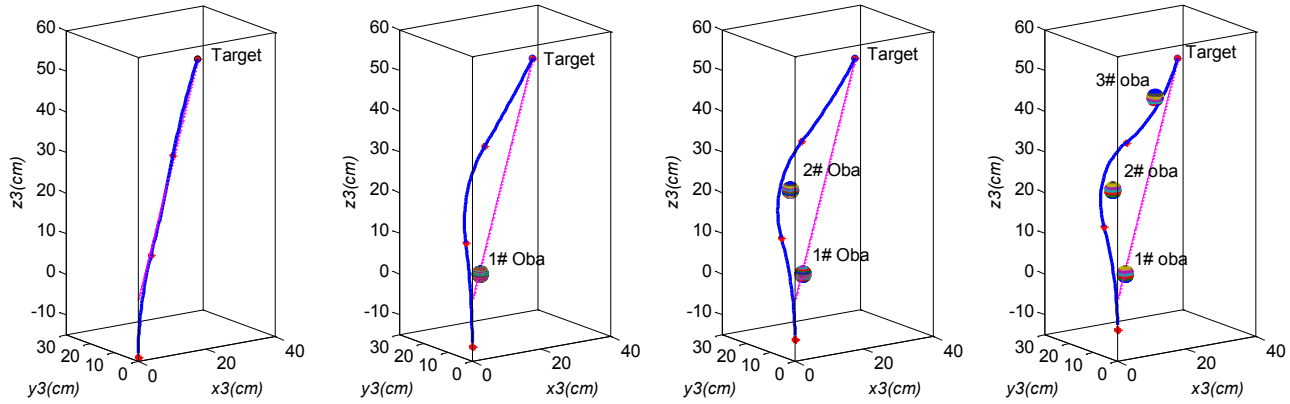

Fig. 6. Simulations of solution paths of three sections while adding an obstacle in succession. The blue curve is path solved, the pink line is the straight reference line, and the red points are endpoints of section. (a) shows a path with an obstacle far from the target and the origin. (b) shows a path avoids 1# obstacle chosen from path in (a). Then 2# obstacle is chosen on path in (b), and the path avoiding two obstacles is depicted in (c). The path with three obstacles is shown in (d) for the same target. All the figures are on the same view.

TABLE II. DATA RESPONSING TO THE SOLUTION PATHS IN FIG. 6.

Fig.6	**Target**	**Obstacles**	**Bending Angles**	**Rotation Angles**	**Rising Distance**	**Tip Point**
			$\{\theta_1,\theta_2,\theta_3\}$(radian)	$\{\varphi_1,\varphi_2,\varphi_3\}$(radian)	*dis*(cm)	
(a)	[30,18,51]	none	{0.62,-0.15, 0.32}	{0.54,0.54, 0.54}	-13.99	[30.01,18.01,51.00]
(b)		1# [3.90,2.25,5.45]	{0.49,0.65,-0.10}	{1.22,6.00,6.79}	-11.34	[30.03,17.95,51.00]
(c)		1# [3.90,2.25,5.45] 2# [6.15,10.67,23.86]	{0.71,0.96,0.57}	{1.35,5.41,1.44}	-9.57	[30.02,17.94,51.00]
(d)		1# [3.90,2.25,5.45] 2# [6.15,10.67,23.86] 3# [21.34,14.93,43.35]	{0.60,1.07,1.13}	{1.42,6.24,3.99}	-7.08	[29.95,17.97,51.00]

B. Results Analysis

Through analysis of given algorithm and corresponding designed simulations, we can get conclusions as follows.

First, based on region clipping search method, a lower time complexity $O(LOOP\times(K\times NUM)^{2N})$ (K is the number of chosen points on the arm, definitions of *LOOP* and *NUM* are given in above sections) is got according to the loops in above tables. We do not give path solved by blind search, for its computing complexity is enormous as $O(N^{2\pi/\Delta\theta})$ if we want to get a same precision as $\Delta\theta$ with the new method. The bigger the N, the more obvious the difference.

Second, when a target and some obstacles are set in the space, we can get a suitable path according to the given algorithm, but another path can be also obtained by adding another section or more, as shown in Fig. 7. The more the number of obstacles is, the more number of sections we need, so we can change the rule of stopping loops in the algorithm, and choose a path with a more appropriate number of sections.

Third, due to the existence of rising distance, we adopt a projection strategy is adopted to simplify the planning problem, but paths above or below obstacles are ignored. It leads to some insoluble cases, for example, when a lot of obstacles distribute around Z-axis and between the origin and the target, there is no path according to the projection strategy, but in fact, there exist paths passing through above or below the obstacles. So, the avoidance strategy has expectations to be improved.

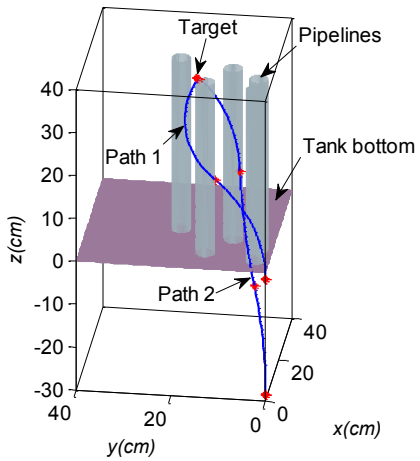

Fig. 7. Different solution paths for a same target by changing the rule of stop loops in the given algorithm, where there are Path 1 of three sections and Path 2 of two sections for a target [19,17,35].

V. Conclusions and Future Work

In this paper, we aim to plan a feasible path as quickly as possible for AFTIR while avoiding obstacles. Path planning of continuum robot is defined firstly. When it comes to avoidance strategy, we formulate the planning problem as a nonlinear constrained optimization and what we need is to solve the problem using a forward search method. We emphasis the improvement on search method, and the search method based on region clipping is presented to reduce computing time complexity. During the planning process, we present a projection strategy through defining target plane zone, target space zone, and obstacle space zone. At the same time, we make a fictitious straight line as an object of reference between the original point and the target point. These methods are used to simplify the planning problem. When the tip of Snake Arm reaches the target plane zone, MDS with reference straight line is calculated to optimize the solutions. Simulations of region clipping and collision free path planning algorithm are carried out to demonstrate excellent performance of the novel search method and feasibility of the planning strategy.

In future work, improvements will be made to adapt special situations and a more congested environment with complex obstacles, that is, the strategy will be more universal. We also plan to apply the strategy to practical experiments of prototype, and an integrated motion planning software to guide users conveniently will be designed.

Acknowledgment

This work was supported by Robotics Institute of Civil Aviation University of China.

References

[1] G. Ch. Niu, Z. Ch. Zheng, Q. J. Gao, W. J. Wang, and L. Wang, "A novel design of aircraft fuel tank inspection robot," *TELKOMNIKA*, vol. 11, no. 7, pp. 3684-3692, July 2013.

[2] R. Buckingham, "Snake arm robots," *Industrial Robot: An International Journal*, vol. 29, no.3, pp. 242-245, 2002.

[3] N. Simaan, "Snake-like units using flexible backbones and actuation redundancy for enhanced miniaturization," in *Proc. IEEE Int. Conf. on Robotics and Automation*, Barcelona, 2005, pp. 3012-3017.

[4] W. McMahan, B. A. Jones, and I. D. Walker, "Design and implementation of a multi-section continuum robot: Air-Octor," in *Pro. IEEE/RSJ Int. Conf. on Intelligent Robots and Systems*, Edmonton, 2005, pp. 3345-3352.

[5] W. McMahan, B. A. Jones, V. Chitrakaran, M. Csencsits, M. Grissom, M. Pritts, C. D. Rahn, and I. D. Walker, "Field trials and testing of the OctArm continuum manipulator," in *Proc. IEEE Int. Conf. on Robotics and Automation*, Orlando, 2006, pp. 2336-2341.

[6] R. J. Webster III, A. M. Okamura, and N. J. Cowan, "Toward active cannulas: miniature snake-like surgical robots," in *Proc. IEEE/RSJ Int. Conf. on Intelligent Robots and Systems*, Beijing, 2006, pp. 2857-2863.

[7] G. Chen, M. T. Pham, and T. Redarce, "Development and kinematic analysis of a silicone-rubber bending tip for colonoscopy," in *Proc. IEEE/RSJ Int. Conf. on Intelligent Robots and Systems*, Beijing, 2006, pp. 168-173.

[8] M. Rolf and J. J. Steil, "Constant curvature continuum kinematics as fast approximate model for the bionic handling assistant," in *2012 IEEE/RSJ Int. Conf. on Intelligent Robots and Systems*, pp. 3440-3446.

[9] Mehling J S, Diftler M A, Chu M, and Valvo, M, "A Minimally invasive tendril robot for in-space inspection", in *the First IEEE/RAS-EMBS Int. Conf. on Biomedical Robotics and Biomechatronics*,2006, pp: 690-695.

[10] Dupont P E, Lock J, Itkowitz B, Evan Butlerl. "Design and control of concentric-tube robots". *IEEE TRANSAC TIONS ON ROBOTICS*, vol.26, no. 2, pp: 209-225,2010.

[11] G. S. Chirikjian and J. W. Burdick, "An obstacle avoidance algorithm for hyper-redundant manipulators," in *1990 IEEE Int. Conf. on Robotics and Automation*, pp. 625–631 vol.1.

[12] L. A. Lyons, R. J. Webster, and R. Alterovitz, "Motion planning for active cannulas," in *2009 IEEE/RSJ Int. Conf. on Intelligent Robots and Systems*, pp. 801–806.

[13] I. S. Godage, D. T. Branson, E. Guglielmino, G. A. Medrano-Cerda, and D. G. Caldwell, "Shape function-based kinematics and dynamics for variable length continuum robotic arms," in *2011 IEEE Int. Conf. on Robotics and Automation*, pp. 452–457.

[14] I. S. Godage, D. T. Branson, E. Guglielmino, and D. G. Caldwell, "Path planning for multisection continuum arms," in *Proc. IEEE Int. Conf. on Mechatronics and Automation*, Chengdu, 2012, pp. 1208-1213.

[15] J. Xiao and R. Vatcha, "Real-time adaptive motion planning for a continuum manipulator," in *2010 IEEE/RSJ Int. Conf. on Intelligent Robots and Systems*, pp. 5919–5926.

[16] V. Duindam, R. Alterovitz, S. Sastry, and K. Goldberg, "Screw-based motion planning for bevel-tip flexible needles in 3D environments with obstacles," in *2008 IEEE Int. Conf. on Robotics and Automation*, pp. 2483-2488.

[17] J. J. Xu, V. Duindam, R. Alterovitz, and K. Goldberg, "Motion planning for steerable needles in 3D environments with obstacles using rapidly-exploring random trees and backchaining," in *4th IEEE Conf. on Automation Science and Engineering*, 2008, pp. 41-46.

[18] R. Alterovitz, T. Simeon, and K. Goldberg, "The stochastic motion road map: a sampling framework for planning with Markov motion uncertainty," *Robotics: Science and Systems III*, pp: 246-253, 2007.

[19] L. G. Torres and R. Alterovitz, "Motion planning for concentric tube robots using mechanics-based models", in *2011 IEEE/RSJ Int. Conf. on Intelligent Robots and Systems*, San Francisco, 2011, pp: 5153-5159.

[20] Q. J. Gao, L. Wang, G.Ch. Niu and W. J. Wang, "Path planning for continuum robot based on target guided angle," *Beijing Hangkong Hangtian Daxue Xuebao/Journal of Beijing University of Aeronautics and Astronautics*, vol. 39, no. 11, pp. 1486-1490, November 2013.

[21] W. Rudin, *Principles of Mathematical Analysis* (Third Edition), USA: McGraw-Hill, Inc, 1976, pp. 83-97.